Ferromagnetic transition of a spin-orbit coupled dipolar Fermi gas at finite temperature

Xue-Jing Feng(冯雪景), Lan Yin(尹澜)

Citation: Chin. Phys. B . 2020, 29(11): 110306 . **doi:** 10.1088/1674-1056/aba9ca
Journal homepage: http://cpb.iphy.ac.cn; http://iopscience.iop.org/cpb

What follows is a list of articles you may be interested in

Lattice configurations in spin-1 Bose-Einstein condensates with the SU(3) spin-orbit coupling

Ji-Guo Wang(王继国), Yue-Qing Li(李月晴), Yu-Fei Dong(董雨菲)

Chin. Phys. B . 2020, 29(10): 100304 . **doi:** 10.1088/1674-1056/abab72

Landau-like quantized levels of neutral atom induced by a dark-soliton shaped electric field

Yueming Wang(王月明), Zhen Jin(靳祯)

Chin. Phys. B . 2020, 29(1): 010303 . **doi:** 10.1088/1674-1056/ab5938

SU(3) spin-orbit-coupled Bose-Einstein condensate confined in a harmonic plus quartic trap

Hao Li(李昊), Fanglin Chen(陈方林)

Chin. Phys. B . 2019, 28(7): 070302 . **doi:** 10.1088/1674-1056/28/7/070302

Topological superfluid in a two-dimensional polarized Fermi gas with spin-orbit coupling and adiabatic rotation

Lei Qiao(乔雷), Cheng Chi(迟诚)

Chin. Phys. B . 2017, 26(12): 120304 . **doi:** 10.1088/1674-1056/26/12/120304

Tunable ground-state solitons in spin-orbit coupling Bose-Einstein condensates in the presence of optical lattices

Huafeng Zhang(张华峰), Fang Chen(陈方), Chunchao Yu(郁春潮), Lihui Sun(孙利辉), Dahai Xu(徐大海)

Chin. Phys. B . 2017, 26(8): 080304 . **doi:** 10.1088/1674-1056/26/8/080304

RAPID COMMUNICATION

Ferromagnetic transition of a spin–orbit coupled dipolar Fermi gas at finite temperature*

Xue-Jing Feng(冯雪景) and Lan Yin(尹澜)†

School of Physics, Peking University, Beijing 100871, *China*

(Received 15 May 2020; revised manuscript received 29 June 2020; accepted manuscript online 28 July 2020)

We study the ferromagnetic transition of a two-component homogeneous dipolar Fermi gas with 1D spin–orbit coupling (SOC) at finite temperature. The ferromagnetic transition temperature is obtained as functions of dipolar constant $\lambda_{\rm d}$, spin–orbit coupling constant $\lambda_{\rm SOC}$ and contact interaction constant $\lambda_{\rm s}$. It increases monotonically with these three parameters. In the ferromagnetic phase, the Fermi surfaces of different components can be deformed differently. The phase diagrams at finite temperature are obtained.

Keywords: dipolar Fermi gas, stoner model, spin–orbit coupling

PACS: 03.75.Ss, 67.85.–d, 67.85.Lm, 05.30.Fk **DOI:** 10.1088/1674-1056/aba9ca

Since the realization of Bose–Einstein condensation in alkali atoms,[1,2] there are many breakthroughs in the field of ultracold atoms, among which the creation of ultracold dipolar gas in polar molecules ^{40}K^{87}Rb,[3–6] ^{23}Na^{40}K[7] and magnetic dipolar atoms ^{161}Dy[8] are striking. Due to the anisotropy and long range character of the dipolar interaction, unconventional quantum phases such as p-wave or d-wave superfluidity,[9–18] supersolidity[19–21] and charge density wave[22,23] were predicted in dipolar Fermi gases. Raman-induced artificial spin–orbit coupling (SOC) has been realized in the dysprosium system,[24] which stimulates our research of the spin–orbit coupled dipolar system.

Experimental search for the itinerant ferromagnetism state[25,26] in a two-component Fermi gas has been intriguing since Stoner published his theory.[27,28] Up to date, most theoretical studies on the itinerant ferromagnetism have been restricted to the case with an s-wave contact interaction,[29–35] although fluctuation effects were considered using different methods. Several papers studied the formation of itinerant ferromagnetism in the presence of repulsive polaron.[34,35] The ferromagnetic state can be formed with less contact interaction in the presence of a magnetic dipolar interaction.[36] When 1D SOC is added to a two-component dipolar Fermi gas it shows in our previous work that the system undergoes a 1st-order and 2nd-order transition from a paramagnetic state to a ferromagnetic state at zero temperature.[37] In this paper we investigate the spin–orbit coupled dipolar Fermi system at finite temperature using the self-consistent Hartree–Fock approximation to determine the ferromagnetic transition temperature and finite-temperature phase diagram.

The Hamiltonian for the two-component dipolar Fermi system in the momentum space consists of three parts, the kinetic energy part $H_{\rm kin}$, the 1D SOC part $H_{\rm SOC}$, and the interaction part $H_{\rm I}$ which includes both dipole–dipole interaction and contact potential,

$$H_{\rm kin} = \sum_{\boldsymbol{k}\alpha} \frac{\hbar^2 k^2}{2m} a^+_{\boldsymbol{k}\alpha} a_{\boldsymbol{k}\alpha}, \tag{1}$$

$$H_{\rm SOC} = \sum_{\boldsymbol{k}\alpha\alpha'} \frac{\hbar^2 k_0}{m} k_z \sigma^z_{\alpha\alpha'} a^+_{\boldsymbol{k}\alpha'} a_{\boldsymbol{k}\alpha}, \tag{2}$$

$$H_{\rm I} = \sum_{\boldsymbol{k}\boldsymbol{k}'\boldsymbol{q}} \sum_{\alpha\alpha'\beta\beta'} \left[\frac{2\pi d^2}{3V} \sigma^i_{\alpha\alpha'} (3\hat{\boldsymbol{q}}_i \hat{\boldsymbol{q}}_j - \delta_{ij}) \sigma^j_{\beta\beta'} + \frac{g}{2V} \delta_{\alpha\alpha'} \delta_{\beta\beta'} \right] a^+_{\boldsymbol{k}+\boldsymbol{q}\alpha} a^+_{\boldsymbol{k}'-\boldsymbol{q}\beta} a_{\boldsymbol{k}'\beta'} a_{\boldsymbol{k}\alpha'}, \tag{3}$$

where $a^+_{\boldsymbol{k}\alpha}$ and $a_{\boldsymbol{k}\alpha}$ are the fermion creation and annihilation operators, the spin-up and spin-down components are labeled with $\alpha = 1, 2$ respectively, indexes i, j, k all represent x, y, z directions, σ^i represents the Pauli matrix, d is the dipole moment of the fermion, g is the coupling constant of the contact interaction, and k_0 is the SOC strength.

In the Hartree–Fock approximation, we obtain excitation energies of spin-up and spin-down atoms

$$\varepsilon_1(\boldsymbol{k}) = \frac{\hbar^2 k^2}{2m} + \frac{\hbar^2 k_0 k_z}{m} + \frac{g}{V} \sum_{\boldsymbol{k}'} n_{2\boldsymbol{k}'} + \frac{4\pi d^2}{3V} \sum_{\boldsymbol{k}'} (3\cos^2\theta_{\boldsymbol{k}-\boldsymbol{k}'} - 1)(n_{2\boldsymbol{k}'} - n_{1\boldsymbol{k}'}), \tag{4}$$

$$\varepsilon_2(\boldsymbol{k}) = \frac{\hbar^2 k^2}{2m} - \frac{\hbar^2 k_0 k_z}{m} + \frac{g}{V} \sum_{\boldsymbol{k}'} n_{1\boldsymbol{k}'} + \frac{4\pi d^2}{3V} \sum_{\boldsymbol{k}'} (3\cos^2\theta_{\boldsymbol{k}-\boldsymbol{k}'} - 1)(n_{1\boldsymbol{k}'} - n_{2\boldsymbol{k}'}), \tag{5}$$

*Project supported by the National Key Research and Development Project of China (Grant No. 2016YFA0301501).

†Corresponding author. E-mail: yinlan@pku.edu.cn

where $\theta_{\boldsymbol{k}-\boldsymbol{k}'}$ is the angle between $\boldsymbol{k}-\boldsymbol{k}'$ and the z axis, and the fermion occupation number is given by

$$n_{\alpha\boldsymbol{k}} = \frac{1}{\mathrm{e}^{[\varepsilon_\alpha(\boldsymbol{k})-\mu]/k_\mathrm{B}T}+1}. \tag{6}$$

The fermion occupation numbers can be solved self-consistently with the constraint on the total number

$$N = \sum_{\boldsymbol{k}}(n_{1\boldsymbol{k}}+n_{2\boldsymbol{k}}). \tag{7}$$

For convenience, we introduce the dimensionless parameters including DDI constant $\lambda_\mathrm{d} = nd^2/\varepsilon_\mathrm{F}$, SOC constant $\lambda_\mathrm{SOC} = k_0/k_\mathrm{F}$, contact interaction constant $\lambda_\mathrm{s} = gn/\varepsilon_\mathrm{F}$, and the temperature constant $\lambda_\mathrm{T} = k_\mathrm{B}T/\varepsilon_\mathrm{F}$, where ε_F is the Fermi energy, k_F is the Fermi wave vector, and k_B is the Boltzmann constant.

In the absence SOC and dipole interaction as in the original Stoner model, only the repulsive s-wave interaction is present, and at the low temperatures the ferromagnetic transition temperature is a function of the contact interaction constant, $\lambda_\mathrm{s} = 4/3 + a_2\lambda_\mathrm{T}^2 + a_4\lambda_\mathrm{T}^4 + \cdots$, where $a_2 = \pi^2/9 = 1.096622$ and $a_4 = \pi^4/20 = 4.870454$. When 1D SOC is added to the Stoner model, Fermi surfaces of two components are translated oppositely in $\boldsymbol{k}$-space by $\pm\boldsymbol{k}_0$ where $\boldsymbol{k}_0 = k_0\hat{\boldsymbol{z}}$. By defining new wavevectors $\boldsymbol{k}' = \boldsymbol{k}+\boldsymbol{k}_0$ for the spin-up component and $\boldsymbol{k}' = \boldsymbol{k}-\boldsymbol{k}_0$ for the spin-down component, the Hamiltonian can be written in the same form as before. Thus SOC does not change the relation between the ferromagnetic transition temperature and the contact interaction. The spontaneous magnetization can occur in any direction in the spin space.

When the dipolar interaction is present, the Hamilonians with and without SOC can no longer be brought in the same form by redefining the wavevectors, because the dipole-dipole interaction is not rotationally invariant in the spin space. The Hamiltonian in the Hartree–Fock approximation can only be diagonalized self-consistently when the magnetization appears in the SOC direction. The SOC enhances ferromagnetism in the presence of the dipolar interaction,[37] which can be seen from the energy difference between the fully magnetized state and the paramagnetic state. With and without SOC, the dipolar interaction energy is the same in the fully magnetized state. However in the paramagnetic state, SOC leads to the relative translation of the two Fermi surfaces. As a result, the dipolar interaction energy between the spin-up and spin-down components is increased because the transferred momentum in this interaction process is shifted by $\pm 2\boldsymbol{k}_0$ and the dipolar interaction strength is increased. Therefore the energy difference between the paramagnetic state and the fully magnetized state is larger in the presence of SOC.

We solve the fermion occupation number self-consistently in the Hartree–Fock approximation, from which the magnetization M can be obtained as

$$M = \frac{1}{N}\sum_{\boldsymbol{k}}(n_{1\boldsymbol{k}} - n_{2\boldsymbol{k}}). \tag{8}$$

The ferromagnetic transition point is where the magnetization M vanishes. As shown in Fig. 1, the magnetization increases monotonically with any one of the three parameters λ_d, λ_SOC, and λ_s above the ferromagnetic transition point with the rest parameters are fixed. When these three parameters are fixed, below the critical temperature the magnetization decreases with the increase in temperature.

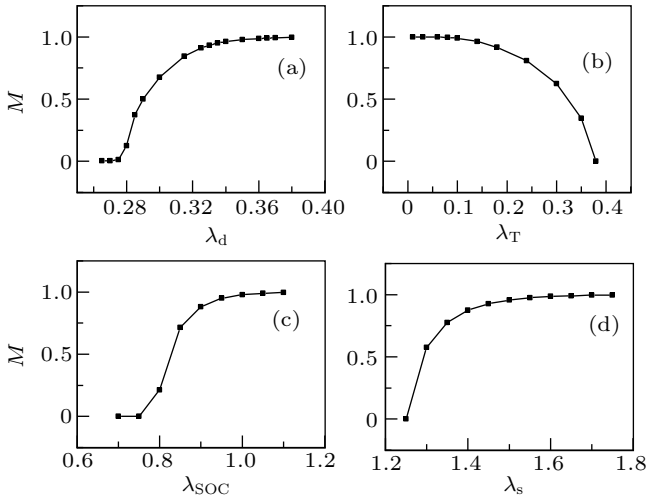

Fig. 1. Magnetization M as functions of λ_d, λ_T, λ_SOC, and λ_s. (a) M increases with λ_d for $\lambda_\mathrm{SOC} = 0.7$, $\lambda_\mathrm{T} = 0.1$ and $\lambda_\mathrm{s} = 0$; (b) M decreases with λ_T for $\lambda_\mathrm{SOC} = 1$, $\lambda_\mathrm{d} = 0.26$ and $\lambda_\mathrm{s} = 0$; (c) M increases with λ_SOC for $\lambda_\mathrm{d} = 0.25$, $\lambda_\mathrm{T} = 0.1$ and $\lambda_\mathrm{s} = 0$; (d) M increases with λ_s for $\lambda_\mathrm{SOC} = 0.6$, $\lambda_\mathrm{d} = 0.02$ and $\lambda_\mathrm{T} = 0.1$.

From the magnetization, we compute the ferromagnetic transition temperature numerically and present it in Fig. 2. The ferromagnetic transition temperature increases with the contact interaction constant λ_s, as shown in Fig. 2(a). The presence of the dipolar interaction and SOC can increase the transition temperature and reduce the critical contact interaction at zero temperature. For fixed λ_s and λ_SOC, the ferromagnetic transition temperature increases monotonically with the dipolar interaction constant λ_d, as shown in Fig. 2(b). For constant λ_s and finite λ_d, the ferromagnetic transition temperature increases with the SOC constant λ_SOC, as shown in Fig. 2(c). In the inset, the ferromagnetic transition temperature shows a saturation behavior when λ_SOC is increased to large values. These results show that the dipolar interaction, contact interaction, and SOC in the presence of the dipolar interaction all enhance ferromagnetism. The increase of the three parameters, λ_d, λ_SOC, and λ_s, all help to stabilize the ferromagnetic state.

We obtain the finite temperature phase diagrams shown in Fig. 3. In the absence of the contact interaction, when λ_SOC and λ_d are relatively small, this system is in the paramagnetic phase, as shown by the solid line in Fig. 3. When λ_SOC and

λ_d increase to critical values, the system goes to the ferromagnetic state. As temperature increases, larger critical values of λ_{SOC} and λ_d are needed for the ferromagnetic phase. When contact interaction is present, the ferromagnetic phase transition takes place at smaller critical values of λ_d and λ_{SOC} as shown by the dotted line Fig. 3.

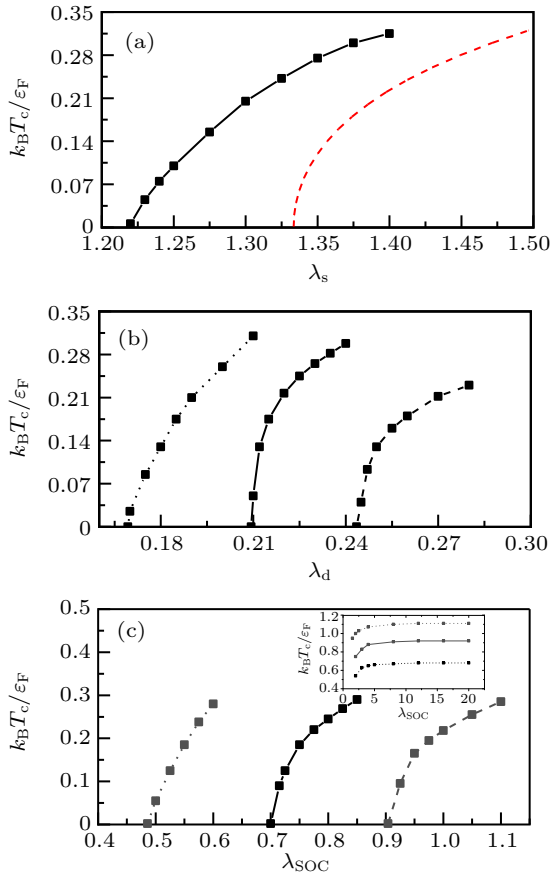

Fig. 2. Ferromagnetic transition temperature as functions of λ_s, λ_d, λ_{SOC}. In (a), the solid line is the ferromagnetic transition temperature as a function of λ_s with $\lambda_{SOC} = 0.6$ and $\lambda_d = 0.02$ and the red dashed line is the result of the Stoner model. In (b), the solid line is the temperature for $\lambda_{SOC} = 1$ and $\lambda_s = 0$. The dashed line is the temperature for $\lambda_{SOC} = 0.8$ and $\lambda_s = 0$. The dotted line is the temperature for $\lambda_{SOC} = 1.0$ and $\lambda_s = 0.2$. In (c), the solid line is the temperature for $\lambda_d = 0.27$ and $\lambda_s = 0$. The dashed line is the temperature for $\lambda_d = 0.22$ and $\lambda_s = 0$. The dotted line is the temperature for $\lambda_d = 0.27$ and $\lambda_s = 0.4$. In the inset, these lines are saturated to different values at large λ_{SOC}.

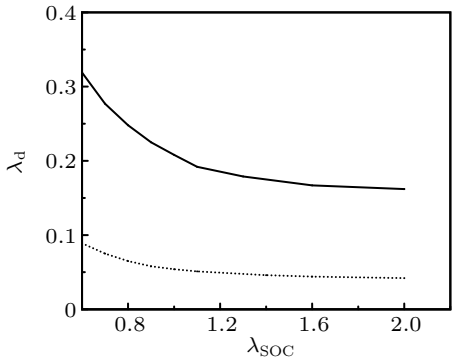

Fig. 3. Phase diagram at $\lambda_T = 0.1$. The horizontal axis represents SOC constant λ_{SOC} and the vertical axis represents DDI constant λ_d. The solid and dotted lines are ferromagnetic transition lines. The solid line is for $\lambda_s = 0$ while the dotted line is for $\lambda_s = 1$.

In a single component dipolar Fermi system at zero temperature, Fermi surface can be elongated along the polarization direction[38,39] and in a two-component system, Fermi surfaces of spin-up and spin-down can be one elongated and one stretched or both elongated.[36,37] To characterize Fermi surfaces at finite temperature, we introduce deformation parameters $\alpha_1 = \langle|k_x|\rangle/\langle|k_z - k_0|\rangle$ for spin-up atoms and $\alpha_2 = \langle|k_x|\rangle/\langle|k_z - k_0|\rangle$ for spin-down atoms. As shown in Fig. 4, the two Fermi surfaces can be deformed differently at low temperatures in the ferromagnetic phase. As temperature increases, the system undergoes a transition to the paramagnetic phase where the deformation of the two Fermi surfaces are the same.

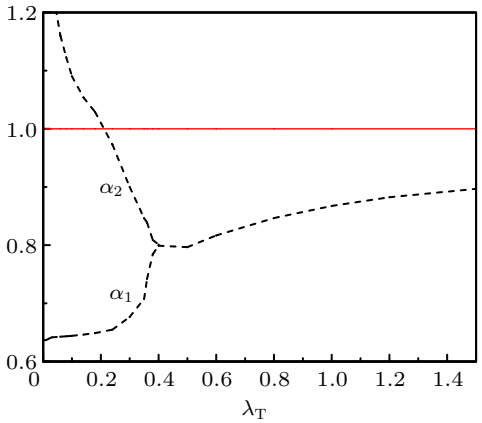

Fig. 4. Parameters α_1 and α_2 as a function of λ_T with $\lambda_{SOC} = 1.0$, $\lambda_d = 0.26$ and $\lambda_s = 0$. As λ_T increases, α_1 and α_2 meet at the ferromagnetic transition temperature and then slowly approach to 1 from below, which indicates that the two Fermi surfaces are deformed differently in the ferromagnetic phase. The red solid line stands for the ideal Fermi surface.

In the experimental system of dipolar ^{161}Dy with SOC,[24] the experimental parameters are given by $\lambda_{SOC} \approx 0.6$, $\lambda_d \approx 0.02$ with density of 10^{14} cm^{-3}, and λ_T ranges from 0.1 to 0.4. In the absence of the s-wave contact interaction, the system is in the normal state at zero temperature according to our results. If the contact interaction can be tuned by Feshbach resonance, with λ_s increasing to about 1.25, the ferromagnetic transition temperature is about 30 nK corresponding to $\lambda_T = 0.1$, which is available in the experiment.

In summary, we have studied the ferromagnetic transition in a spin–orbit coupled two-component dipolar Fermi gas. It is found that the ferromagnetic transition temperature increases with the dipolar and contact interaction, and also SOC strength. The deformations of the two Fermi-surfaces can be different in the Ferromagnetic phase and become the same in the paramagnetic state. Finite-temperature phase diagrams are obtained.

Acknowledgements

We would like to thank Z. Q. Yu and B. Liu for helpful discussions.

References

[1] Anderson M H, Ensher J R, Matthews M R, Wieman C E and Cornell E A 1995 *Science* **269** 198
[2] Davis K B, Mewes M O, Andrews M R, van Druten N J, Durfee D S, Kurn D M and Ketterle W 1995 *Phys. Rev. Lett.* **75** 3969
[3] Ni K K, Ospelkaus S, de Miranda M H G, Pe'Er A, Neyenhuis B, Zirbel J J, Kotochigova S, Julienne P S, Jin D S and Ye J 2008 *Science* **322** 231
[4] Bo Y, Moses S A, Bryce G, Covey J P, Hazzard K R A, Ana Maria R, Jin D S and Jun Y 2013 *Nature* **501** 521
[5] Chotia A, Neyenhuis B, Moses S A, Yan B, Covey J P, Foss-Feig M, Rey A M, Jin D S and Ye J 2012 *Phys. Rev. Lett.* **108** 080405
[6] Ni K K, Ospelkaus S, Wang D, Quéméner G, Neyenhuis B, de Miranda M H G, Bohn J L, Ye J and Jin D S 2010 *Nature* **464** 1324
[7] Wu C H, Park J W, Ahmadi P, Will S and Zwierlein M W 2012 *Phys. Rev. Lett.* **109** 085301
[8] Lu M, Burdick N Q and Lev B L 2012 *Phys. Rev. Lett.* **108** 215301
[9] You L and Marinescu M 1999 *Phys. Rev. A* **60** 2324
[10] Cooper N R and Shlyapnikov G V 2009 *Phys. Rev. Lett.* **103** 155302
[11] Levinsen J, Cooper N R and Shlyapnikov G V 2011 *Phys. Rev. A* **84** 013603
[12] Wu C and Hirsch J E 2010 *Phys. Rev. B* **81** 020508
[13] Pikovski A, Klawunn M, Shlyapnikov G V and Santos L 2010 *Phys. Rev. Lett.* **105** 215302
[14] Gadsbølle A L and Bruun G M 2012 *Phys. Rev. A* **86** 033623
[15] Liu B and Yin L 2012 *Phys. Rev. A* **86** 031603
[16] Liu B and Yin L 2011 *Phys. Rev. A* **84** 043630
[17] Gorshkov A V, Manmana S R, Chen G, Ye J, Demler E, Lukin M D and Rey A M 2011 *Phys. Rev. Lett.* **107** 115301
[18] Liao R and Brand J 2010 *Phys. Rev. A* **82** 063624
[19] Balibar S 2010 *Nature* **464** 176
[20] Zeng T S and Yin L 2014 *Phys. Rev. B* **89** 174511
[21] Zhang Y C, Maucher F and Pohl T 2019 *Phys. Rev. Lett.* **123** 015301
[22] Bhongale S G, Mathey L, Tsai S W, Clark C W and Zhao E 2012 *Phys. Rev. Lett.* **108** 145301
[23] Yamaguchi Y, Sogo T, Ito T and Miyakawa T 2010 *Phys. Rev. A* **82** 013643
[24] Burdick N Q, Tang Y and Lev B L 2016 *Phys. Rev. X* **6** 031022
[25] Jo G B, Lee Y R, Choi J H, Christensen C A, Kim T H, Thywissen J H, Pritchard D E and Ketterle W 2009 *Science* **325** 1521
[26] Valtolina G, Scazza F, Amico A, Burchianti A, Recati A, Enss T, Inguscio M, Zaccanti M and Roati G 2017 *Nat. Phys.* **13** 704
[27] Stoner E C 1938 *Proc. R. Soc. London. Ser. A* **165** 372
[28] Stoner E C 1933 *London Edinburgh Dublin Philos. Mag. J. Sci.* **15** 1018
[29] Duine R A and MacDonald A H 2005 *Phys. Rev. Lett.* **95** 230403
[30] Ryszkiewicz J, Brewczyk M and Karpiuk T 2020 *Phys. Rev. A* **101** 013618
[31] He L, Liu X J, Huang X G and Hu H 2016 *Phys. Rev. A* **93** 063629
[32] Zhai H 2009 *Phys. Rev. A* **80** 051605
[33] Pilati S, Bertaina G, Giorgini S and Troyer M 2010 *Phys. Rev. Lett.* **105** 030405
[34] Deng T S, Lu Z C, Shi Y R, Chen J G, Zhang W and Yi W 2018 *Phys. Rev. A* **97** 013635
[35] Massignan P and Bruun G M 2011 *Eur. Phys. J. D* **65** 83
[36] Fregoso B M and Fradkin E 2009 *Phys. Rev. Lett.* **103** 205301
[37] Feng X J and Yin L 2020 *Chin. Phys. Lett.* **37** 020301
[38] Miyakawa T, Sogo T and Pu H 2008 *Phys. Rev. A* **77** 061603
[39] Ronen S and Bohn J L 2010 *Phys. Rev. A* **81** 033601